

## ARTICLE

# Pre-TCR $\alpha$ supports CD3-dependent reactivation and expansion of TCR $\alpha$ -deficient primary human T-cells

Román Galetto<sup>1</sup>, Celine Lebuhotel<sup>1</sup>, Laurent Poirot<sup>1</sup>, Agnès Gouble<sup>1</sup>, Maria L Toribio<sup>2</sup>, Julianne Smith<sup>1</sup> and Andrew Scharenberg<sup>1</sup>

Chimeric antigen receptor technology offers a highly effective means for increasing the anti-tumor effects of autologous adoptive T-cell immunotherapy, and could be made widely available if adapted to the use of allogeneic T-cells. Although gene-editing technology can be used to remove the alloreactive potential of third party T-cells through destruction of either the  $\alpha$  or  $\beta$  T-cell receptor (TCR) subunit genes, this approach results in the associated loss of surface expression of the CD3 complex. This is nonetheless problematic as it results in the lack of an important trophic signal normally mediated by the CD3 complex at the cell surface, potentially compromising T-cell survival *in vivo*, and eliminating the potential to expand TCR-knockout cells using stimulatory anti-CD3 antibodies. Here, we show that pre-TCR $\alpha$ , a TCR $\alpha$  surrogate that pairs with TCR $\beta$  chains to signal proper TCR $\beta$  folding during T-cell development, can be expressed in TCR $\alpha$  knockout mature T-cells to support CD3 expression at the cell surface. Cells expressing pre-TCR/CD3 complexes can be activated and expanded using standard CD3/CD28 T-cell activation protocols. Thus, heterologous expression of pre-TCR $\alpha$  represents a promising technology for use in the manufacturing of TCR-deficient T-cells for adoptive immunotherapy applications.

*Molecular Therapy — Methods & Clinical Development* (2014) **1**, 14021; doi:10.1038/mtm.2014.21; published online 11 June 2014

## INTRODUCTION

Recent advances in adoptive T-cell immunotherapy and chimeric antigen receptor technology have the potential to revolutionize the way that many kinds of cancer are treated, by enabling a patient's T-cells to be removed from their body, genetically engineered to specifically target their cancer, and transferred back into the patient to eradicate the cancer. To date, this and related advanced adoptive immunotherapies have only been applied on an autologous basis to maximize the potential for the modified T-cells to sustainably engraft following their adoptive transfer back into the patient.<sup>1,2</sup>

The use of major histocompatibility complex (MHC)-mismatched allogeneic donor T-cells would be a less expensive and more easily scalable method for the implementation of engineered T-cell therapies. However, this approach brings with it the potential of both host versus graft and graft versus host (GvH) alloreactivity. Host versus graft alloreactivity leads to short-term engraftment due to host immune responses that eradicate the donor T-cells. Thus, in order for them to be engrafted and therapeutically effective, cells must be administered to highly immunodepleted patients. More serious consequences can arise from GvH alloreactivity, where MHC-mismatched donor T-cells may be driven to expand out of control due to T-cell receptor (TCR)-mismatched MHC interaction, resulting in an aggressive inflammatory response with lethal potential.

Because of the seriousness of MHC-mismatched GvH alloreactivity, before MHC-mismatched allogeneic T-cells can be applied in adoptive immunotherapy, their endogenous TCR specificity

must either be altered or removed entirely.<sup>3,4</sup> Of these two options, removing TCR specificity is simpler, as it requires disruption of either the TCR $\alpha$  or the TCR $\beta$  genes, whereas altering the TCR specificity requires sequential disruption and replacement of both genes. However, disruption of a single TCR subunit gene without replacement is accompanied by the loss of CD3 expression at the cell surface. This loss is a significant issue, as the presence of the TCR/CD3 complex on the cell surface provides a trophic signal, which is important for the survival of many types of effector T-cells. Thus, loss of surface CD3 would be predicted to substantially compromise the survival of adoptively transferred TCR-deficient T-cells. A second issue of considerable practical importance is that the manufacturing of off-the-shelf T-cells would most straightforwardly be accomplished through the use of CD3/CD28 co-stimulation technology, which depends on T-cell activation via the TCR/CD3 complex.

To address the issues associated with loss of surface CD3 complexes upon TCR $\alpha$  gene disruption, we hypothesized that the expression of pre-TCR $\alpha$ , a surrogate partner for properly folded TCR $\beta$  chains during T-cell development,<sup>5-7</sup> would be able to pair with all  $\beta$  chains expressed in a T-cell population, and support surface CD3 expression through a pre-TCR/CD3 complex (Figure 1a, upper panel). These complexes are transiently expressed during normal thymocyte development at the  $\beta$  selection step, and are thought to generate a ligand-independent signal.<sup>8,9</sup> This signal induces expansion and maturation of developing pre-T-cells into CD4<sup>+</sup>CD8<sup>+</sup> double-positive thymocytes, and TCR $\alpha$  gene rearrangement, resulting

<sup>1</sup>Cellectis Therapeutics, Paris, France; <sup>2</sup>Centro de Biología Molecular Severo Ochoa, Consejo Superior de Investigaciones Científicas, Universidad Autónoma de Madrid, Madrid, Spain. Correspondence: Andrew Scharenberg (scharenberg@cellectis.com) or Julianne Smith (smith@cellectis.com)

Received 11 February 2014; accepted 28 April 2014

in the substitution of pre-TCR $\alpha$  by TCR $\alpha$  chains, subsequent TCR $\alpha\beta$  selection, and final differentiation into conventional single-positive thymocytes.<sup>10-13</sup>

To test if pre-TCR $\alpha$  expression could reconstitute surface expression of CD3 following TCR $\alpha$  disruption, we generated a TCR $\alpha$ -deficient Jurkat T-cell line using transcription activator-like effector nucleases (TALENs) and evaluated a series of pre-TCR $\alpha$  constructs. Of those tested, we found that a previously described pre-TCR $\alpha$ - $\Delta$ 48 truncation mutant<sup>14</sup> supported the highest level of surface CD3

expression. Furthermore, heterologous expression of pre-TCR $\alpha$  in TCR-deficient primary T-cells restored their competence for activation via CD3/CD28 stimulation, resulting in enhanced survival properties, superior cell expansion potential, and the capacity for pre-TCR/CD3-mediated cytotoxic T-cell degranulation. Taken together, our results indicate that heterologous pre-TCR $\alpha$  expression can be used to replace a disrupted TCR $\alpha$  gene, providing a new tool for use in the development of "off-the-shelf" adoptive T-cell immunotherapies based on TCR $\alpha$  gene disrupted cells.

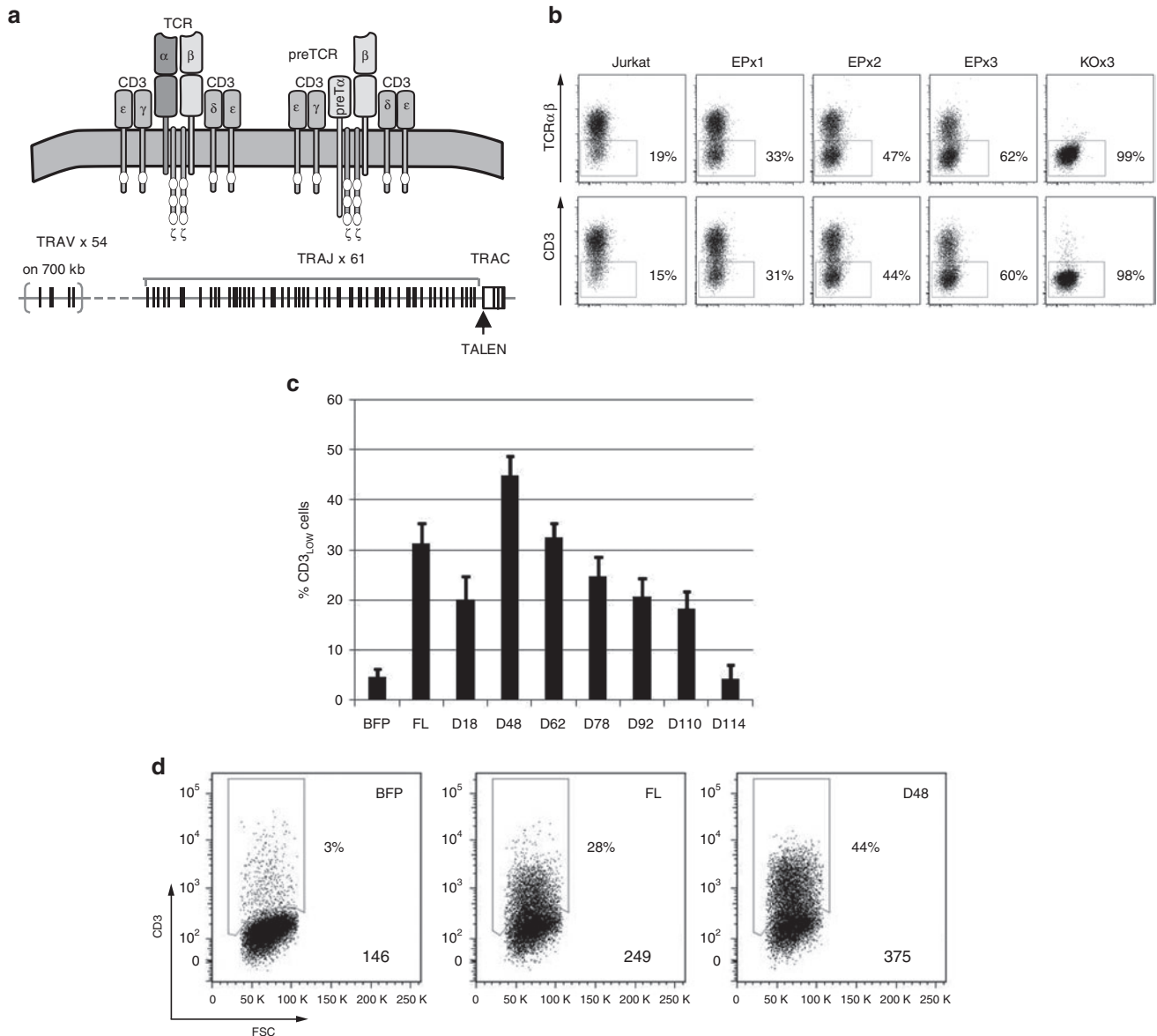


**Figure 1** Screening of pre-TCR $\alpha$  constructs in TCR $\alpha$  deficient Jurkat cells. **(a)** represents the multi-component TCR $\alpha\beta$  and pre-TCR complexes as assembled at the cell surface. The TCR $\alpha$  genomic locus (TRA) is shown in the lower part of the panel, with the arrangement of the variable (V), joining (J) and constant (C) gene segments, as well as the position targeted by the transcription activator-like effector nuclease (TALEN) used to generate the TCR $\alpha$  disrupted cells. **(b)** Flow cytometry data from the generation of TCR $\alpha$  KO Jurkat cells upon three consecutive transfections (EPx1, EPx2, and EPx3) of the plasmids coding for TALEN targeting exon 1 of the TCR $\alpha$  chain constant region. The right-most flow panel (KOx3) shows TCR $\alpha\beta$  and CD3 staining of the TCR $\alpha$  KO Jurkat cells after purification of the CD3<sub>NEG</sub> population. **(c)** The percentage of cells in which CD3 restoration (CD3<sub>LOW</sub>) is observed upon transfection of pre-TCR $\alpha$  variants harboring different truncations in the cytoplasmic tail. The name of each construct corresponds to the number of residues eliminated from the C-terminus of the cytoplasmic tail. As a negative control, data of cells transfected with a plasmid encoding blue fluorescent protein (BFP) under the control of the same promoter as the pre-TCR $\alpha$  variants is shown (by using this plasmid, transfection efficiency was determined in each experiment, which was always >90%). Transfections had been carried out in at least three independent experiments for each construct. **(d)** An example of flow cytometry data from the pre-TCR $\alpha$ -FL and D48 variants. The geometrical mean fluorescence intensity (MFI) of the CD3 signal is shown for the whole cell population in each case, for a single representative experiment, in the lower-right corner of each flow panel.

## RESULTS

Screening of pre-TCR $\alpha$  constructs to identify optimal variants supporting CD3 expression

**Generation of TCR-deficient Jurkat T-cells by TALEN gene editing.** In order to generate a model for evaluation of pre-TCR $\alpha$  mediated restoration of CD3 expression, we utilized TALEN gene editing technology to knockout (KO) the TCR $\alpha$  gene in Jurkat tumor T-cells. Upon generation of a double strand break (DSB) within the TALEN target sequence, permanent gene inactivation is achieved via repair by nonhomologous end joining at this DSB, through nucleotide deletion or insertion at the cleaved site.<sup>15,16</sup> TALENs designed to cleave the first exon of the TCR $\alpha$  constant region (Figure 1a, lower panel) were expressed in Jurkat T-cells using a plasmid driving TALEN expression of an EF1 $\alpha$  promoter. Following a series of three sequential electroporations, the population of Jurkat cells had shifted from approximately 19% TCR $\alpha\beta$ -negative (Figure 1b, Jurkat flow panel) to approximately 60% TCR $\alpha\beta$ -negative (EPx3 flow panel), suggesting that the TCR $\alpha$  locus had been successfully disrupted in a high fraction of the population. This was correlated to a loss of CD3 surface expression, as shown in the lower line of the flow data presented in Figure 1b. The CD3-negative population was subsequently isolated by negative selection with CD3-coated magnetic beads (Figure 1b, KOx3 flow panel) and expanded for further use in assessing the influence of pre-TCR $\alpha$  on CD3 surface expression.

**Heterologous transient expression of pre-TCR $\alpha$  constructs in TCR $\alpha$  deficient Jurkat T-cells.** Human pre-TCR $\alpha$  comprises a single

immunoglobulin-like domain linked by a connecting peptide to a transmembrane region and a cytoplasmic tail (114 amino acids) that is considerably longer than that of the standard TCR $\alpha$  chains.<sup>17,18</sup> When associated with TCR $\beta$ , an interchain disulfide bond is mediated through a Cys residue present in the connecting peptide,<sup>14</sup> while the association of the pre-TCR $\alpha$ /TCR $\beta$  dimer with signal-transducing CD3 molecules is achieved similarly to a conventional TCR, through residues in the transmembrane span.<sup>19</sup> The cytoplasmic tail harbors domains regulating pre-TCR $\alpha$  surface expression, including an apparent endoplasmic reticulum retention signal, and a second sequence mediating constitutive internalization and degradation.<sup>20–22</sup> In addition, potential protein kinase C phosphorylation sites, a CD2-like domain and a proline-rich motif that could potentially be involved in signal transduction are also present in the intracellular domain.<sup>14,17</sup>

Expression of full length human pre-TCR $\alpha$  has been shown to generate low levels of surface CD3 expression<sup>14,18</sup> and constitutive internalization of pre-TCR/CD3 complexes; however, truncated forms of pre-TCR $\alpha$ , in particular a variant with 48 amino acids deleted from the C-terminal cytoplasmic tail, have been reported to support higher levels of CD3 expression and reduced constitutive internalization.<sup>14,20</sup> To identify a form of pre-TCR $\alpha$  capable of supporting the highest level of CD3 surface expression, we transfected a series of pre-TCR $\alpha$  truncation variants (full length to a tail-less -D114- version, see Figure 1c) into the TCR $\alpha$ -deficient Jurkat cell model, and labeled the resulting cell populations with an anti-CD3 antibody 48 hours after transfection. We observed that the pre-TCR $\alpha$ -D48 variant was able to support the highest level of CD3 surface expression, followed by the full length pre-TCR $\alpha$  and pre-TCR $\alpha$ -D62 variants, for both of which CD3

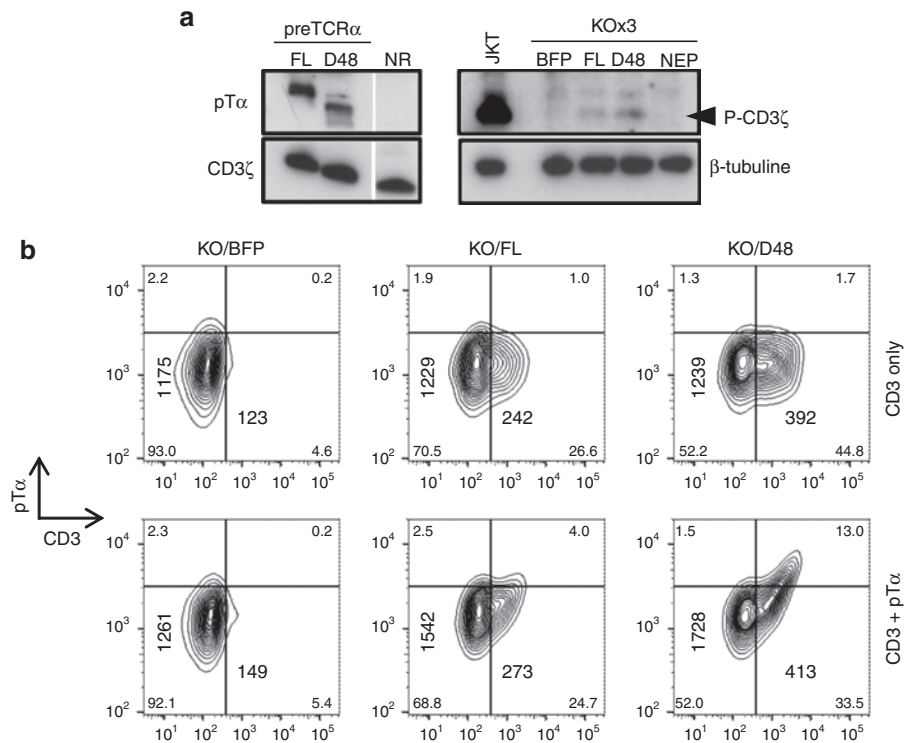


**Figure 2** Pre-TCR $\alpha$  expression and signaling capacity in TCR $\alpha$  disrupted Jurkat cells. Detection of pre-TCR $\alpha$ -FL and -D48 by (a) Western blot (WB) (left blot) and (b) flow cytometry 48 hours after transfection, showing that pre-TCR $\alpha$  expression levels correlate with those of CD3 restoration. Nonrelated (NR): cells transfected with a nonrelated plasmid; BFP: cells transfected with a BFP encoding plasmid. The right blot of panel a show the phosphorylation status of CD3 $\zeta$  chains on Jurkat and in TCR $\alpha$  edited cells (KOx3) 48 hours after transfection with a BFP, pre-TCR $\alpha$ -FL or pre-TCR $\alpha$ -D48 encoding plasmid, and of non electroporated (NEP) cells. (b) Flow data of KOx3 Jurkat cells transfected with the BFP, pre-TCR $\alpha$ -FL or pre-TCR $\alpha$ -D48 expression plasmids and stained with anti-CD3 or anti-CD3 plus anti-pre-TCR $\alpha$  antibodies. The MFIs of CD3 and pre-TCR $\alpha$  signals are shown in the corresponding axes for the global cell population.

expression was approximately 50% lower (Figure 1c). Flow data for CD3 expression are shown for the FL and D48 pre-TCR $\alpha$  versions in Figure 1d, compared to cells transfected with a blue fluorescent protein (BFP) expression plasmid. The BFP expression plasmid was also used to monitor transfection efficiencies, which were consistently >90% in all the independent experiments (not shown).

Pre-TCR $\alpha$ /CD3 complexes expressed at the surface of TCR $\alpha$  deficient cells can transduce cell activation signals

Protein expression of pre-TCR $\alpha$  was confirmed by western blot (Figure 2a, left blot) using a polyclonal antibody targeting the extracellular domain of pre-TCR $\alpha$  (residues 61–82). In addition, flow cytometry was carried out to detect pre-TCR $\alpha$  at the cell surface

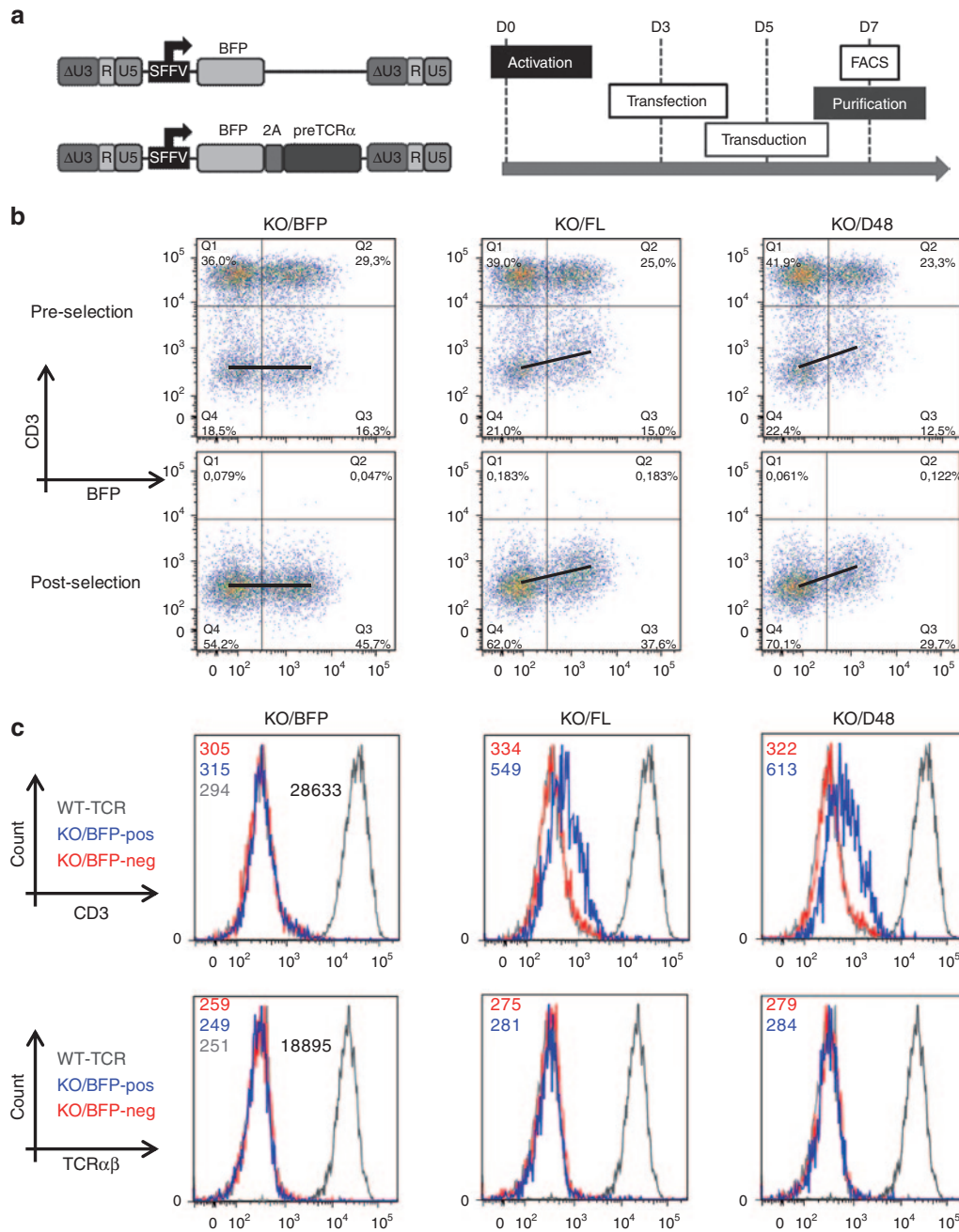


**Figure 3** Pre-TCR $\alpha$  mediated restoration of surface CD3 expression in TCR $\alpha$  KO primary T-cells. A schema of the lentiviral vectors used for pre-TCR $\alpha$  expression, together with the experimental plan are depicted in panel **a**. T-cells are purified from buffy-coat and activated at day 0 (D0), followed by transcription activator-like effector nuclease (TALEN) mRNA transfection (D3), lentiviral transduction (D5), and enrichment of TCR $\alpha$  disrupted cells (D7). The bicistronic lentiviral vectors allow the discrimination of pre-TCR $\alpha$  expressing cells by flow cytometry, based on the BFP signal. FACS analysis for BFP and CD3 expression at D7 are shown before and after depletion of CD3 positive cells (panel **b**, upper and lower rows, respectively). **(c)** The levels of CD3 and TCR $\alpha\beta$  expression in TCR $\alpha$  KO cells transduced with the control BFP or with the BFP-2A-pre-TCR $\alpha$ -FL or -D48 rLV vectors, gated on the BFP(+) (blue histograms) or BFP(-) (red histograms) populations. The light-gray histograms correspond to CD3 and TCR $\alpha\beta$  signals from non transduced TCR $\alpha$  deficient T-cells. All the cells that had been transfected with the TRAC TALEN followed the same purification protocol 4 days after transfection. The dark-gray histograms correspond to CD3 and TCR $\alpha\beta$  signals obtained in non transfected T-cells from the same donor (WT, wild type). The values showed in each condition represent the MFI data for each population analyzed in a representative experiment. The color code is the same for the histograms and the MFI values. Experiments were carried out at least four times.

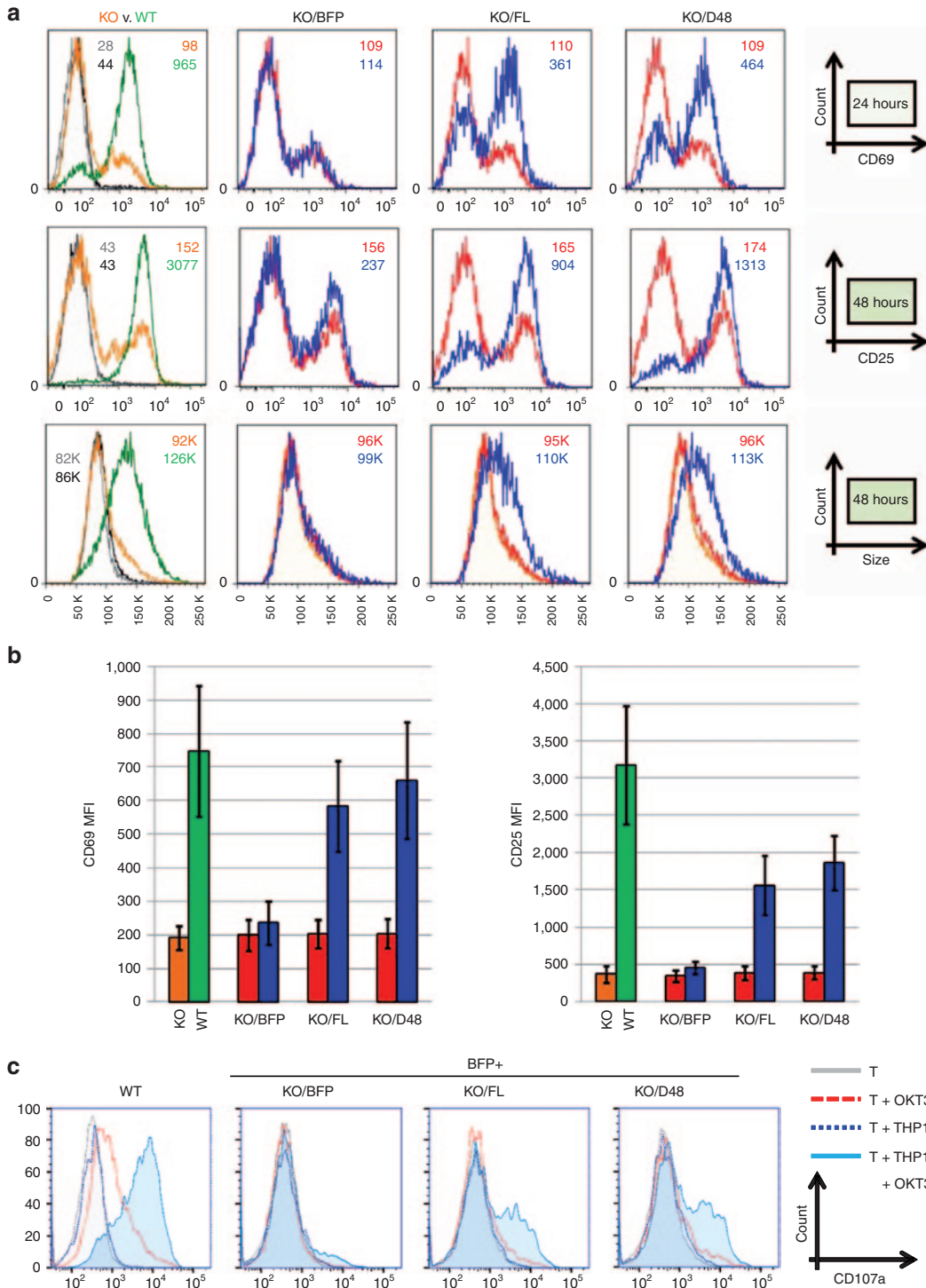
using the K5G3 monoclonal antibody<sup>23</sup> (targeting also the extra-cellular domain), which allowed us to correlate pre-TCR $\alpha$  and CD3 expression upon double staining of the transfected cells (Figure 2b).

Since the pre-TCR complex has been proposed to mediate autonomous signaling through dimerization on the cell surface,<sup>8,24</sup> we evaluated the degree of phosphorylation of the CD3zeta chain (CD3 $\zeta$ ) in transfected cells by western blot using an anti-phospho-CD3 $\zeta$  antibody. The WB presented on the right panel of Figure 2a shows that no phosphorylation is observed in TCR $\alpha$  KO cells transfected with a control plasmid encoding the BFP, while it is detected in TCR $\alpha$  KO cells transfected with pre-TCR $\alpha$  encoding plasmids, either the FL

or D48 variants. Although these phospho-zeta signals were weaker than those observed in nongenetically modified Jurkat cells, consistent with the much higher levels of TCR $\alpha\beta$  complexes at the cell membrane compared to those of pre-TCR complex in this cellular model, these results nevertheless indicate that pre-TCR $\alpha$ /CD3 complexes are competent for transducing cell activation signals.

Pre-TCR $\alpha$  can support CD3 expression in TCR-deficient primary T-cells

Based on the results from the expression of pre-TCR $\alpha$  variants in TCR $\alpha$  deficient Jurkat T-cells, we developed lentiviral vector



constructs driving expression of BFP followed by a 2A ribosomal skip peptide and full length pre-TCR $\alpha$  or pre-TCR $\alpha$ -D48 variants. A schema of the expression vectors is shown in Figure 3a, together with that of the control vector, expressing BFP but not pre-TCR $\alpha$ .

To determine if transduction of pre-TCR $\alpha$  variants (-FL and -D48) could support the surface expression of CD3 in TCR-deficient primary human T-cells, we purified T-cells from buffy-coat samples and activated them on CD3/CD28 beads for 72 hours. Cells were then electroporated with mRNA encoding TCR $\alpha$ -targeting TALEN (the same used for generating TCR $\alpha$  deficient Jurkat cells), and transduced them 48 hours later with lentiviral vectors driving expression of BFP alone, or BFP-2A-pre-TCR $\alpha$ -FL or -D48. The resulting cell populations were analyzed by flow cytometry 48 hours following transduction and TCR $\alpha$  disrupted cells were purified by negative selection on CD3-coated magnetic beads (Figure 3a, experimental scheme).

TALEN mRNA transfection led to efficient TCR $\alpha$  gene disruption in primary T-cells, with gene knockout frequencies ranging from 30 to 50% among different donors. When these cells were transduced with the BFP-only control vector, we did not detect any impact on CD3 expression levels, while BFP-2A-pre-TCR $\alpha$ -FL or -D48 expressing cells supported a clearly detectable CD3 surface expression above baseline level (CD3<sub>LOW</sub> cells) in TCR $\alpha$  KO cells. Results from a representative donor are shown in Figure 3b (upper row). The low levels of CD3 restoration observed are compatible with the expected low levels of pre-TCR $\alpha$  expression,<sup>25</sup> and both CD3<sub>NEG</sub> and CD3<sub>LOW</sub> populations could therefore be recovered together upon depletion of cells expressing physiological levels of CD3 (Figure 3b, lower row). The results are even clearer when analyzing TCR $\alpha\beta$  negative enriched cells by gating on the BFP(+) or BFP(-) cells to evaluate CD3 expression (Figure 3c, blue and red histograms, respectively). Staining of the same cells with an anti-TCR $\alpha\beta$  antibody did not yield any signal, either in BFP(+) or BFP(-) cells (Figure 3c, lower row), indicating that the CD3 signals observed in BFP(+) cells are specific for pre-TCR complexes. Based on these data, we conclude that pre-TCR $\alpha$  pairs with the endogenous TCR $\beta$  genes in TCR $\alpha$ -gene disrupted cells, and results in surface expression of a pre-TCR $\alpha$ /TCR $\beta$ /CD3 complex (hereafter designated as pre-TCR/CD3 complex). In addition, we show that in TCR $\alpha$  disrupted primary T-cells, the pre-TCR $\alpha$ -D48 variant might allow a greater number of pre-TCR/CD3 complexes to be expressed at the cell surface, consistent with the results obtained in TCR $\alpha$  knockout Jurkat cells.

#### Pre-TCR $\alpha$ -mediated CD3 expression supports activation of TCR-deficient primary T-cells

To determine if pre-TCR/CD3 complexes were able to transduce cell activation signals in TCR $\alpha$  disrupted primary T-cells, we analyzed the

expression of activation markers CD69 and CD25 following exposure of cells to anti-CD3 and anti-CD28 antibodies (Figure 4). As shown in Figure 4a (first and second row), BFP positive cells expressing pre-TCR/CD3 complexes demonstrated upregulation of CD69 and CD25 at 24 and 48 hours, respectively, following stimulation with CD3/CD28 beads, though to a lesser extent than in the control TCR $\alpha\beta$  expressing cells (WT cells in the figure). Cell size was also analyzed following exposure to CD3/CD28 beads, as a measure of the competence of the pre-TCR/CD3 complexes to induce “blasting” (Figure 4a, third row). Stimulation with CD3/CD28 beads induced comparable increases in cell size in cells expressing TCR $\alpha\beta$ /CD3 complexes versus cells expressing pre-TCR/CD3 complexes. Consistently, the responses tend to correlate with the CD3 restoration levels observed in cells expressing pre-TCR $\alpha$ -D48 or pre-TCR $\alpha$ -FL, as illustrated, for example, via assessment of MFI of activation markers on T-cells isolated from four different donors (Figure 4b).

To further evaluate the capacity of pre-TCR/CD3 complexes to mediate T-cell activation, we used a cell-based anti-CD3 cytotoxicity assay to determine their capacity to induce cytotoxic granule exocytosis. The human monocytic cell line THP-1, which expresses Fc receptors, was co-cultured with TCR $\alpha$  KO T-cells, expressing or not pre-TCR $\alpha$ , in the presence or not of the anti-CD3 antibody OKT3. Cells were co-cultured for 6 hours and stained for surface expression of CD107a, a marker of cytotoxic T-cell granule exocytosis. The results show that pre-TCR $\alpha$  expressing cells co-cultured with THP-1 cells exhibit degranulation activity only in the presence of the OKT3 antibody (Figure 4c). Furthermore, co-culturing T-cells with KOx3 cells (which do not express CD3, neither Fc receptors) showed no surface mobilization of CD107a (not shown). Also, TCR $\alpha$  KO T-cells lacking pre-TCR $\alpha$  expression showed no degranulation in any of the conditions tested. Taken together, these results suggest that pre-TCR/CD3 complexes are competent to transduce signals permitting efficient activation marker upregulation and can induce degranulation, in a manner qualitatively indistinguishable from that generated by a TCR $\alpha\beta$ /CD3 complex.

#### Pre-TCR $\alpha$ -mediated CD3 expression supports survival and expansion of TCR-deficient primary T-cells upon stimulation with CD3 antibodies

To evaluate the capacity of pre-TCR/CD3 complexes to support longer-term cell proliferation, we generated mixed populations of TCR $\alpha$  disrupted T-cells expressing or not pre-TCR/CD3 complexes, and reactivated them 5 days posttransduction using CD3/CD28 beads and IL-2. Following reactivation, we monitored the expansion of the cell populations cultured for up to a 25 day period. Cells

**Figure 4** Expression of activation markers upon treatment with CD3/CD28 beads. (a), flow data of cells stained for detection of the CD69 and CD25 activation markers, measured at 24 or 48 hours after reactivation with CD3/CD28 beads, respectively. Cell size (forward scatter) was also determined 48 hours after reactivation (third row). Blue and red histograms are the signals from TCR $\alpha$  KO T-cells gated on the BFP(+) or BFP(-) cell populations, respectively. The orange histograms correspond to signals obtained upon reactivation of nontransduced TCR $\alpha$  KO T-cells. Green histograms correspond to TCR $\alpha\beta$  expressing cells from the same donor (non transfected cells, WT). Black and gray histograms in the first column correspond to TCR $\alpha\beta$ (+) or nontransduced TCR $\alpha$  KO cells that were not reactivated with CD3/CD28 beads. The values shown in each of the flow graphs are the MFIs of each of the populations analyzed, using the same color code described before. Data shown correspond to a representative donor among four different donors analyzed. (b) The MFI for CD69 and CD25 signals on reactivated TCR $\alpha$  KO cells for four independent donors. The orange bars correspond to signals obtained upon reactivation of purified TCR $\alpha$  KO cells, while green bars represent the signals obtained in reactivated TCR $\alpha$  positive cells from the same donor. In the three remaining groups, the red and blue bars correspond to signals obtained from BFP(-) or BFP(+) cells, respectively, upon reactivation. For all the samples that had been transfected with TRAC transcription activator-like effector nuclease (TALEN) mRNA, TCR $\alpha$  knockout cells have been purified by negative selection with CD3 magnetic beads, as depicted in Figure 3. (c) The CD107a mobilization induced upon engagement of effector toward target cells through a soluble antibody. The histograms show the CD107a signal in different populations of viable CD8+ T-cells and following different activation conditions. Basal signals are shown in gray, while those obtained upon incubation with the anti-CD3 (OKT3) antibody alone are shown as a red dashed histogram. Signals corresponding to co-cultures of T-cells with THP-1 are represented as blue dotted lines, and co-cultures of T-cells with THP-1 in the presence of OKT3 are shown as a shaded light-blue histogram. For TCR $\alpha$  KO cells, only the results observed on BFP(+) cells are shown, since no differences were observed on BFP(-) cells, which showed no CD107a mobilization in any of the conditions tested. All the populations yielded the same levels of positive signals upon activation with phorbol myristate acetate and ionomycin, while incubation of any of the cellular populations with Jurkat KOx3 cells (which do not express Fc receptors) showed no degranulation activity in the presence or not of soluble OKT3 (not shown).

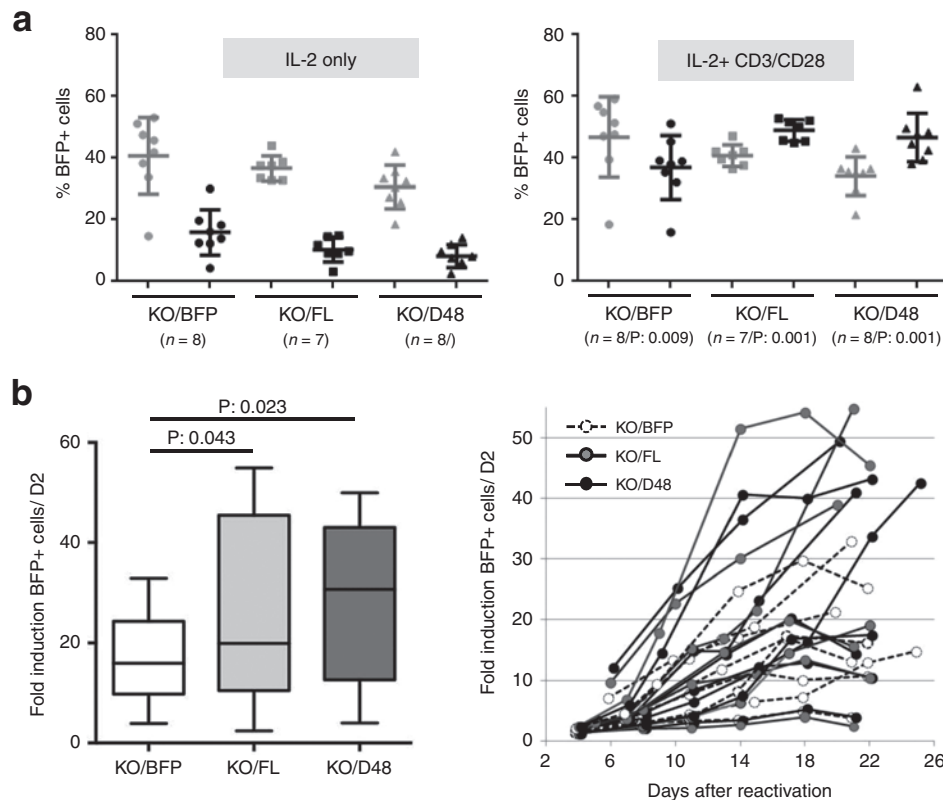


**Figure 5** Expansion of TCR $\alpha$  KO BFP(+) cells upon reactivation with CD3/CD28 beads. **(a)** The percentage of BFP(+) cells when they have been reactivated with CD3/CD28 beads (right panel) or kept in culture in the presence of IL-2 only (left panel). TCR $\alpha$  KO cells transduced with the BFP control vector are shown as circles, while cells expressing pre-TCR $\alpha$ -FL or pre-TCR $\alpha$ -D48 as squares or triangles, respectively. Dataset in gray represents the values observed 48 hours after the reactivation step, while those in black are the values observed at the end of the experiment. Mean  $\pm$  SD values are represented. The *P* values obtained when comparing percentages of BFP(+) cells at the beginning and end of experiment are given for each of the reactivated samples. **(b)** The fold induction in the number of BFP(+) cells at the end of the experiment with respect to those 48 hours after reactivation with CD3/CD28 beads (left panel). The horizontal line represents the median value of each dataset. The mean values are 16.9; 26.9 and 28.8 for the KO/BFP, KO/FL and KO/D48 samples, respectively. The curves in the right panel represent the growth kinetics of the different donors, in terms of fold induction in the number of BFP(+) cells at each timepoint respect to the amount of BFP(+) cells at D2.

were analyzed by flow cytometry every 3–5 days and the number of BFP(+) cells was determined at each time.

As the expansion kinetics of each donor were different, we compared the percentage of BFP(+) cells early after reactivation (48 hours) to those observed at a late stage of the experiment (17–25 days after reactivation, corresponding to the time point at which the maximum percentage of BFP(+) cells were observed). These data are shown in Figure 5a. The two panels correspond to TCR $\alpha$  disrupted cells grown on IL-2 only (left panel) or reactivated with CD3/CD28 beads (right panel), after transduction with either the BFP-only control vector or with the -FL or -D48 pre-TCR $\alpha$  expressing vectors. The dataset in gray corresponds to signals 48 hours after reactivation, while those in black are those at late stages of the experiment. Importantly, we observed a decrease in the percentage of BFP(+) cells over time in all samples when they were maintained on IL-2 alone, demonstrating that pre-T does not generate a constitutive growth signal capable of driving autonomous cell proliferation in a minimally trophic environment, and that such culture conditions lead to a gradual silencing of transgene expression as the cells move into quiescence. However, when cells were reactivated with CD3/CD28 beads, we observed a decrease in the percentage of BFP(+) cells in controls, but an increase in all cases where cells were expressing any of the pre-TCR $\alpha$  variants. These results indicate that TCR $\alpha$  KO cells expressing pre-TCR/CD3 complexes receive enhanced pro-survival signals when exposed to CD3/CD28 beads,

and are able to survive and expand to a higher degree than cells transduced with the control BFP vector.

This interpretation is further supported by comparisons of the number of BFP(+) cells obtained at the “late” stage of the proliferation experiments vs. those observed 48 hours after reactivation. The data represented in Figure 5b (left panel) show a higher dispersion for cells expressing pre-TCR $\alpha$  than for those expressing only the BFP. A mean fold induction of 26.9 and 28.8 was observed for cells expressing pre-TCR $\alpha$ -FL or -D48, against a 16.9-fold induction observed for the control cells. The right panel of Figure 5b shows the expansion kinetics upon reactivation of the different donors tested over time, highlighting the degree of donor-dependent variability in the proliferative responses to CD3-driven reactivation. The same data is represented for each individual donor in Supplementary Figure S1. The phenotype of engineered and TCR $\alpha\beta$ (+) cells was also determined for one of the donors, showing that no major differences were observed when cells were either kept on IL-2 or reactivated using CD3/CD28 beads (Supplementary Figure S2).

## DISCUSSION

In this study, we show that the heterologous expression of pre-TCR $\alpha$ , a natural partner for TCR $\beta$  chains during T-cell development, can be used to restore CD3 surface expression in human primary T-cells rendered TCR-deficient by TCR $\alpha$  gene disruption. Importantly, pre-TCR/CD3 complexes created by the heterologous pre-TCR $\alpha$  expression

are able to support enhanced survival of TCR-deficient T-cells, and can be used to expand TCR-deficient T-cells using CD3/CD28 T-cell activation protocols.

We evaluated a series of pre-TCR $\alpha$  constructs based on previously published reports regarding human pre-TCR $\alpha$  variants capable of restoring CD3 surface expression.<sup>14,20</sup> Similar to what was previously reported, while multiple truncated variants of pre-TCR $\alpha$  appeared able to support limited amounts of pre-TCR/CD3 surface complexes, a pre-TCR $\alpha$  construct possessing a 48 amino acid deletion from the C-terminus of the intracytoplasmic tail (pre-TCR $\alpha$ - $\Delta$ 48) consistently yielded the highest level of CD3 surface expression. In addition to supporting CD3 surface expression, pre-TCR $\alpha$ -48 as well as WT pre-TCR $\alpha$ -FL were able to support CD3/CD28 bead dependent T-cell activation, granting them improved survival characteristics, as shown by the enrichment of pre-TCR $\alpha$  expressing cells upon reactivation (Figure 5). The impact of pre-TCR $\alpha$  on cell expansion is more difficult to evaluate, as a considerable degree of inter-donor variability is observed in the expansion kinetics. Nevertheless, we observed a clear tendency toward improved doubling capacity in cells expressing pre-TCR/CD3 complexes in comparison to those transduced with a BFP-only control vector. The response of CD3/CD28 reactivation of TCR $\alpha$  KO cells (KO/BFP) suggests that in this experimental context, signaling through CD28 alone is able to provide a pro-proliferative signal; although we have not further explored this phenomenon in the present work. Finally, we evaluated the potential for graft versus host disease (GvHD) development by TCR $\alpha$  knockout cells expressing pre-TCR $\alpha$  constructs in a NOG mouse xenograft model (see Supplementary Table S1 and Supplementary Materials and Methods), and did not observe any evidence of GvHD. Although only a small number of animals were tested in this initial experiment, the complete lack of GvHD observed in pre-T-expressing cells strongly suggests that the pre-Ta constructs evaluated here are not capable of supporting allogeneic immune responses toward an MHC-mismatched host.

In both Jurkat and primary T-cells, we consistently observed higher levels of pre-TCR $\alpha$ -D48/CD3 complex surface expression versus pre-TCR $\alpha$ -FL. Although pre-TCR $\alpha$ -D48 and pre-TCR $\alpha$ -FL displayed only slight differences in cell activation following anti-CD3 stimulation, and similar levels of proliferation following CD3/CD28 bead stimulation, we believe that the ability of pre-TCR $\alpha$ -D48 to support a higher level of CD3 expression may be an important advantage versus pre-TCR $\alpha$ -FL, as increased pre-TCR $\alpha$ /CD3 expression would be predicted to result in higher ligation-independent trophic signaling, as well as a higher potential for pre-TCR $\alpha$ -D48 to be utilized in conjunction with bi-specific reagents in allogeneic immunotherapy approaches. Ligand-independent signaling of pre-TCR/CD3 complexes may also have an important role in supporting signals mediated by chimeric antigen receptors (CARs). The degree of constitutive activity induced by CD19 CARs and the abundance of CD19 expressing cells have been suggested as important correlates of the survival and expansion properties of CD19 CAR T-cells.<sup>26,27</sup> For CARs with lower constitutive activity, or those targeting less abundant antigens, ligand-independent signaling created via pre-TCR/CD3 complexes could play a similarly important role in extending the lifespan of adoptively transferred cells. The impact of pre-TCR $\alpha$  expression might therefore be different for each CAR and its use may therefore be envisioned as conditional on the signaling properties of each individual CAR.

In summary, gene editing of the TCR $\alpha$  locus to eliminate TCR $\alpha$  expression allows the generation of TCR-deficient primary human T-cells. However, TCR-deficient T-cells may lack many physiological signals mediated by surface expression of TCR/CD3 complexes, and are not amenable to manufacturing protocols that utilize CD3/CD28

stimulation to drive T-cell expansion. The results presented here demonstrate that heterologous expression of pre-TCR $\alpha$  or its -D48 variant are able to support surface expression of signaling competent pre-TCR/CD3 complexes in primary human T-cells. We propose that pre-TCR/CD3 reconstitution is a simple and practical method for use in conjunction with TCR $\alpha$  disruption for development and manufacturing of TCR-deficient adoptive T-cell immunotherapies for applications in cancer and infectious diseases.

## MATERIALS AND METHODS

### Generation of TCR-deficient Jurkat cells

TCR deficient Jurkat cells were derived from Jurkat cells (obtained from DMSZ, Germany) using TALEN targeting the constant region of the TCR $\alpha$  gene (produced by Collectis Bioresearch, France), and cloned in plasmids containing a T7 or an EF1-alpha promoter. The target sequence for TRAC TALEN is TTGTCCACAGATATCCagaacctgaccctgCCGTGTACCAGCTGAGA, where the two 17 base pair recognition sites (upper case letters) are separated by a 15-bp spacer (lower case letters).

Cells were cultured at 37 °C with 5% CO<sub>2</sub> in RPMI-1640 media (PAA Laboratories, Austria) supplemented with 10% fetal bovine serum, penicillin (100 IU/ml) and streptomycin (100 µg/ml). For gene disruption, 1 × 10<sup>6</sup> Jurkat cells were electroporated with 15 µg of each of the two TALEN-encoding plasmids using Cytopulse Technology. Cells were electroporated in 0.4 cm gap cuvettes (Bio-Rad Laboratories, Hercules, California) in a final volume of 200 µl of "Cytoporation buffer T" (BTX Harvard Apparatus, Holliston, Massachusetts). The electroporation parameters had been previously optimized and the final protocol consists of two 0.1 mS pulses at 2,000V/cm, followed by four 0.2 mS pulses at 325V/cm. Cells were immediately diluted in complete media and incubated at 37 °C. Three sequential electroporations were done with a 4-days interval between each, in order to maximize the amount of TCR $\alpha$ β negative cells. CD3 negative cells were purified by negative selection using "Human CD3 Microbeads" and "LD columns" (Miltenyi Biotech, Köln, Germany) according to manufacturer's instructions. To determine the knockdown rate and confirm the TCR $\alpha$ β/CD3 negative population purity, cells were labeled with fluorophore-conjugated antibodies against TCR $\alpha$ /β and CD3 (Miltenyi Biotech, Köln, Germany).

### Screening of pre-TCR $\alpha$ variants in TCR $\alpha$ deficient Jurkat cells

To address the effect of transient expression of the different pre-TCR $\alpha$  variants, 1 × 10<sup>6</sup> TCR $\alpha$  deficient Jurkat cells (KOx3) were electroporated with 15 µg of each of the pre-TCR $\alpha$  encoding plasmids, using the same electroporation protocol described above. CD3 surface expression was monitored 48 hours after electroporation, by labeling the cells with a PE-conjugated anti-CD3 antibody (Miltenyi Biotech, Köln, Germany) and detected by flow cytometry.

### Pre-TCR $\alpha$ expression and signaling in TCR-deficient Jurkat cells

Protein extraction from KOx3 cells was done 48 hours after transfection. 25 µg of protein extracts were loaded on SDS-page gels for analysis of pre-TCR $\alpha$  expression by western blot. Blotted membranes were probed with a polyclonal anti-pre-TCR $\alpha$  antibody obtained from rabbit immunization with a peptide comprising residues 61–82 (contained in the pre-TCR $\alpha$  extracellular domain) and an HRP-conjugated secondary antibody. Detection was done using "Supersignal West Femto detection kit" (Thermo Fisher Scientific, Waltham, Massachusetts). For detection of the phosphorylated CD3ζ polypeptide by western blot, the anti-CD247(pY142) antibody (BD Biosciences, San Jose, California) was used. Loading control was done with either an anti-CD3ζ (BD Biosciences, San Jose, California) or anti-β-tubulin antibody (Cell Signaling Technology, Danvers, Massachusetts).

Detection of pre-TCR $\alpha$  on the cell surface was also done 48 hours after electroporation by co-staining of KOx3 cells with anti-pre-TCR $\alpha$  K5G3 antibody (CSIC, Spain) and an APC-conjugated secondary antibody (BD Biosciences, San Jose, California), together with an anti-CD3 PE-conjugated antibody (Miltenyi Biotech, Köln, Germany).

### Primary T-cells

T-cells were purified from buffy-coat samples provided by EFS (Etablissement Français du Sang, Paris, France) using Ficoll gradient density medium (Ficoll Paque PLUS / GE Healthcare Life Sciences, Piscataway, New Jersey). The peripheral blood mononuclear cell layer was recovered and T-cells were purified using the "Human T-cell Enrichment kit"



(Stem Cell Technologies, Vancouver, Canada). Purified T-cells were activated in X-Vivo-15 medium (Lonza, Basel, Switzerland) supplemented with 20 ng/ml Human IL-2 (Miltenyi Biotech, Köln, Germany), 5% human serum (Sera Laboratories, West Sussex, UK), and dynabeads human T activator CD3/CD28 at a bead:cell ratio 1:1 (Life Technologies, Carlsbad, California). 3 days later, beads were removed and 5 million of cells were transfected with 10  $\mu$ g of mRNA of each of the two TALEN targeting the TCR $\alpha$  constant chain (the same used for generating KOx3 Jurkat cells). TALEN mRNAs were produced using the mMESSAGING MACHINES T7 Kit (Life Technologies, Carlsbad, California) and purified using RNeasy Mini Spin Columns (Qiagen, Hilden, Germany). Transfection was done, as for Jurkat cells, using Cytopulse technology, by applying two 0.1 mS pulses at 3,000V/cm followed by four 0.2 mS pulses at 325V/cm in 0.4 cm gap cuvettes in a final volume of 200  $\mu$ l of "Cytoporation buffer T" (BTX Harvard Apparatus, Holliston, Massachusetts). Cells were immediately diluted in X-Vivo-15 media and incubated at 37 °C with 5% CO<sub>2</sub>. IL-2 was added 2 hours after electroporation at 20 ng/ml. The day after transfection, cells were diluted at 1  $\times$  10<sup>6</sup>/ml, and transduced 24 hours later with lentiviral vectors harboring a BFP transgene, or BFP-2A-pre-TCR $\alpha$ -FL or -D48 cassettes, at the multiplicity of infection required for comparable transduction efficiencies (determined by the % of BFP(+) cells).

TCR $\alpha$  knockout and transduction efficiencies were determined by flow cytometry two days after transduction, and CD3 negative cells were purified by negative selection using "Human CD3 Microbeads" and "LD Columns" (Miltenyi Biotech, Köln, Germany). To determine the knockdown rate and confirm the CD3 negative population purity, cells were labeled with fluorophore-conjugated antibodies against TCR $\alpha$ / $\beta$  and CD3 (Miltenyi Biotech, Köln, Germany).

For reactivation experiments, TCR $\alpha$  KO cells were treated with "dynabeads human T activator CD3/CD28" beads (Life Technologies, Carlsbad, California) 3 days after purification, at bead:cell ratio 1:6. A replicate of the same cells was kept in IL-2/X-Vivo-15 media to compare growth rate of reactivated and non reactivated cells. Nonelectroporated cells from the same donor were used as positive control for reactivation marker upregulation. Cells were labeled with APC-conjugated anti-CD69 and anti-CD25 antibodies (Miltenyi Biotech, Köln, Germany) 24 hours and 48 hours after reactivation, respectively. Cells were diluted, supplemented with fresh IL-2 and counted twice a week for at least a 25 day period after reactivation. The amount of BFP(+) cells was also determined at each of these time-points by flow cytometry.

#### CD107a mobilization assay

T-cells were incubated in 96-well plates (80,000 cells/well), together with an equal amount of THP-1 or KOx3 cells, in the presence or not of functional grade anti-CD3 (clone OKT3, Miltenyi Biotech, Köln, Germany) at a concentration of 7.5  $\mu$ g/ml. Co-cultures were maintained in a final volume of 100  $\mu$ l of X-Vivo-15 medium (Lonza, Basel, Switzerland) for 6 hours at 37 °C with 5% CO<sub>2</sub>. CD107a staining was done during cell stimulation, by the addition of an APC-conjugated anti-CD107a antibody (BD Biosciences, San Jose, California) at the beginning of the co-culture, together with 1  $\mu$ g/ml of anti-CD49d (BD Biosciences, San Jose, California), 1  $\mu$ g/ml of anti-CD28 (Miltenyi Biotech, Köln, Germany), and 1 $\times$  Monensin solution (eBioscience, San Diego, California). After the 6 hours incubation period, cells were stained with a fixable viability dye (eBioscience, San Diego, California) and PE-conjugated anti-CD8 (Miltenyi Biotech, Köln, Germany) and analyzed by flow cytometry.

#### Statistical analysis

P values were calculated doing paired t-tests performed using GraphPad Prism version 6.00 for Windows (GraphPad Software, La Jolla CA USA; www.graphpad.com).

#### CONFLICT OF INTEREST

M.L.T. has been supported by the Spanish Ministry of Science and Innovation (grant: SAF2010-15106). The rest of the authors are all employees of Cellectis Therapeutics.

#### REFERENCES

- Kershaw, MH, Westwood, JA and Darcy, PK (2013). Gene-engineered T cells for cancer therapy. *Nat Rev Cancer* **13**: 525–541.
- Restifo, NP, Dudley, ME and Rosenberg, SA (2012). Adoptive immunotherapy for cancer: harnessing the T cell response. *Nat Rev Immunol* **12**: 269–281.
- Provasi, E, Genovese, P, Lombardo, A, Magnani, Z, Liu, PQ, Reik, A et al. (2012). Editing T cell specificity towards leukemia by zinc finger nucleases and lentiviral gene transfer. *Nat Med* **18**: 807–815.

Supplementary Information accompanies this paper on the *Molecular Therapy—Methods & Clinical Development* website (<http://www.nature.com/mtm>)

- Okamoto, S, Mineno, J, Ikeda, H, Fujiwara, H, Yasukawa, M, Shiku, H et al. (2009). Improved expression and reactivity of transduced tumor-specific TCRs in human lymphocytes by specific silencing of endogenous TCR. *Cancer Res* **69**: 9003–9011.
- von Boehmer, H and Fehling, HJ (1997). Structure and function of the pre-T cell receptor. *Annu Rev Immunol* **15**: 433–452.
- Groettrup, M, Ungewiss, K, Azogui, O, Palacios, R, Owen, MJ, Hayday, AC et al. (1993). A novel disulfide-linked heterodimer on pre-T cells consists of the T cell receptor beta chain and a 33 kd glycoprotein. *Cell* **75**: 283–294.
- Saint-Ruf, C, Ungewiss, K, Groettrup, M, Bruno, L, Fehling, HJ and von Boehmer, H (1994). Analysis and expression of a cloned pre-T cell receptor gene. *Science* **266**: 1208–1212.
- Yamasaki, S, Ishikawa, E, Sakuma, M, Ogata, K, Sakata-Sogawa, K, Hiroshima, M et al. (2006). Mechanistic basis of pre-T cell receptor-mediated autonomous signaling critical for thymocyte development. *Nat Immunol* **7**: 67–75.
- Yamasaki, S and Saito, T (2007). Molecular basis for pre-TCR-mediated autonomous signaling. *Trends Immunol* **28**: 39–43.
- Dudley, EC, Petrie, HT, Shah, LM, Owen, MJ and Hayday, AC (1994). T cell receptor beta chain gene rearrangement and selection during thymocyte development in adult mice. *Immunity* **1**: 83–93.
- Aifantis, I, Buer, J, von Boehmer, H and Azogui, O (1997). Essential role of the pre-T cell receptor in allelic exclusion of the T cell receptor beta locus. *Immunity* **7**: 601–607.
- von Boehmer, H, Aifantis, I, Feinberg, J, Lechner, O, Saint-Ruf, C, Walter, U et al. (1999). Pleiotropic changes controlled by the pre-T-cell receptor. *Curr Opin Immunol* **11**: 135–142.
- Kruisbeek, AM, Haks, MC, Carleton, M, Michie, AM, Zúñiga-Pflücker, JC and Wiest, DL (2000). Branching out to gain control: how the pre-TCR is linked to multiple functions. *Immunol Today* **21**: 637–644.
- Carrasco, YR, Navarro, MN, de Yébenes, VG, Ramiro, AR and Toribio, ML (2002). Regulation of surface expression of the human pre-T cell receptor complex. *Semin Immunol* **14**: 325–334.
- Christian, M, Cermak, T, Doyle, EL, Schmidt, C, Zhang, F, Hummel, A et al. (2010). Targeting DNA double-strand breaks with TAL effector nucleases. *Genetics* **186**: 757–761.
- Miller, JC, Tan, S, Qiao, G, Barlow, KA, Wang, J, Xia, DF et al. (2011). A TALE nuclease architecture for efficient genome editing. *Nat Biotechnol* **29**: 143–148.
- Del Porto, P, Bruno, L, Mattei, MG, von Boehmer, H and Saint-Ruf, C (1995). Cloning and comparative analysis of the human pre-T-cell receptor alpha-chain gene. *Proc Natl Acad Sci USA* **92**: 12105–12109.
- Ramiro, AR, Trigueros, C, Márquez, C, San Millán, JL and Toribio, ML (1996). Regulation of pre-T cell receptor (pT alpha-TCR beta) gene expression during human thymic development. *J Exp Med* **184**: 519–530.
- von Boehmer, H (2005). Unique features of the pre-T-cell receptor alpha-chain: not just a surrogate. *Nat Rev Immunol* **5**: 571–577.
- Carrasco, YR, Ramiro, AR, Trigueros, C, de Yébenes, VG, García-Peydró, M and Toribio, ML (2001). An endoplasmic reticulum retention function for the cytoplasmic tail of the human pre-T-cell receptor (TCR) alpha chain: potential role in the regulation of cell surface preTCR expression levels. *J Exp Med* **193**: 1045–1058.
- Panigada, M, Porcellini, S, Barbier, E, Hoeflinger, S, Cazenave, PA, Gu, H et al. (2002). Constitutive endocytosis and degradation of the pre-T cell receptor. *J Exp Med* **195**: 1585–1597.
- Carrasco, YR, Navarro, MN and Toribio, ML (2003). A role for the cytoplasmic tail of the pre-T cell receptor (TCR) alpha chain in promoting constitutive internalization and degradation of the pre-TCR. *J Biol Chem* **278**: 14507–14513.
- Ramiro, AR, Navarro, MN, Carreira, A, Carrasco, YR, de Yébenes, VG, Carrillo, G, et al. (2001). Differential developmental regulation and functional effects on pre-TCR surface expression of human pTalpha(a) and pTalpha(b) spliced isoforms. *J Immunol* **167**: 5106–5114.
- Pang, SS, Berry, R, Chen, Z, Kjer-Nielsen, L, Perugini, MA, King, GF et al. (2010). The structural basis for autonomous dimerization of the pre-T-cell antigen receptor. *Nature* **467**: 844–848.
- Trigueros, C, Ramiro, AR, Carrasco, YR, de Yébenes, VG, Albar, JP and Toribio, ML (1998). Identification of a late stage of small noncycling pTalpha- pre-T cells as immediate precursors of T cell receptor alpha/beta+ thymocytes. *J Exp Med* **188**: 1401–1412.
- Milone, MC, Fish, JD, Carpenito, C, Carroll, RG, Binder, GK, Teachey, D, et al. (2009). Chimeric receptors containing CD137 signal transduction domains mediate enhanced survival of T cells and increased antileukemic efficacy *in vivo*. *Mol Ther* **17**: 1453–1464.
- Kalos, M, Levine, BL, Porter, DL, Katz, S, Grupp, SA, Bagg, A et al. (2011). T cells with chimeric antigen receptors have potent antitumor effects and can establish memory in patients with advanced leukemia. *Sci Transl Med* **3**: 95ra73.



This work is licensed under a Creative Commons Attribution-NonCommercial-NoDerivs 3.0 Unported License. The images or other third party material in this article are included in the article's Creative Commons license, unless indicated otherwise in the credit line; if the material is not included under the Creative Commons license, users will need to obtain permission from the license holder to reproduce the material. To view a copy of this license, visit <http://creativecommons.org/licenses/by-nc-nd/3.0/>